Evaluation of Wear Properties of Heat-Treated Al-AlB$_2$ in-situ Metal Matrix Composites

Samuel Dayanand[1,5] · Satish Babu Boppana[2] · Virupaxi Auradi[3] · Madeva Nagaral[4] · M. Udaya Ravi[2] · Bharath[3]

Abstract

Considerable improvement in weight reduction, strength, wear obstruction, and modulus is the basic in meeting the plan and design criteria for the production of airplane, launch vehicles, and automobiles. This work proposes the low-cost manufacture process involving 2, 4, and 6 wt% AlB$_2$ in-situ particle strengthened with aluminum (Al) Metal Matrix Composites (MMCs) utilizing chemical reaction through exothermic response between halide salt KBF$_4$ and Al matrix at a temperature of 850 °C through vortex technique. The as-cast matrix blend and the in-situ composite were heat treated at a temperature of 535 °C for 1 h accompanied by quenching in various media like ice, oil, and water. The quenched samples were subjected to artificial aging at a temperature of 175 °C for 10 h. Microstructural studies were conducted on the as-cast and in-situ composites for dissemination of AlB$_2$ particles in the as-cast matrix. SEM images affirm the development of AlB$_2$ with uniform circulation in the matrix. X-ray diffractometer test was performed for the formation of AlB$_2$ reinforcement phase in the matrix composite. Wear and mechanical properties were explored for the in-situ composites; for wear test, the impact of sliding rate, applied load, and sliding distance were basic parameters corresponding to the wear experienced by the material. The wear conduct and worn morphology of the aluminum MMCs subjected to various quenchants were additionally evaluated using pin-on-disc tests involving specimens to slide against a hardened steel disc under different load conditions. The exploratory outcomes exhibited that the typical load and fortification proportions were significant variables affecting the volumetric wear rate for all the quenched samples, trailed by sliding speed. The wear resistance behavior is found to be higher for specimens involving ice quenching treatment followed by water and oil-quenched composites.

Keywords AlB$_2$ · in-situ · Halide salt · AMMC · Stir casting

1 Introduction

Aluminum Metal Matrix Composites (AMMCs) fortified with ceramic particulates have been widely used in the aviation and automobile business sectors on account of their high stiffness, low coefficient thermal expansion (CTE), great wear resistance, and solidarity-to-weight proportion [1, 2]. The particulate fortifications added to the unadulterated aluminum incorporate include B$_4$C, Al$_2$O$_3$, SiC, TiB$_2$, and SiO$_2$. Among all the fortifications, boride particles were selected due to their low density and hardness strength [3–6]. Researchers reported that boride particulate-fortified AMMCs can be manufactured through different preparing strategies, for example, fluid state technique and powder metallurgy. Very less research work has been carried out to evaluate the wear behavior of AlB$_2$ particulate-strengthened AMMCs in the as-cast and heat-treated conditions. It is known that AlB$_2$ particulates are viable nucleation locales for aluminum (Al) combinations and the substance's reactivity among particulates and melt is limited, prompting good interfacial holding with the matrix [7, 8]. It is notable that in-situ fortifications offer numerous acceptable favorable circumstances, for example, it provides clean and clear interface and higher holding strength within the matrix. The finer

✉ Samuel Dayanand
samueldayanand@gmail.com

1 Department of Mechanical Engineering, Government Engineering College, Raichur, Karnataka, India

2 Department of Mechanical Engineering, School of Engineering, Presidency University, Bengaluru, Karnataka, India

3 Department of Mechanical Engineering, Siddaganga Institute of Technology, Tumkur, Karnataka, India

4 Aircraft Research and Design Centre, Hindustan Aeronautics Limited, Bengaluru, Karnataka, India

5 VTU, Belagavi, Karnataka, India

particulates also improved properties related to mechanical strength. in-situ ceramic mixes of reinforcement namely TiB_2, Al_2O_3, ZrB_2, and TiC have been widely utilized as fortifications in AMMCs. In practical applications, the sliding velocity and applied normal load influence the rate of wear of composite materials in automobile and aerospace sectors [9, 10]. The wear rate increases with increasing load and speed. The composites with higher reinforcement content offer considerable resistance to wear. Further, the hardness strength of the matrix also plays an important role in acting against wear [11–13].

The process of heat treatment improves the surface properties of the materials. The hardness strength of the composites is generally found to improve with the heat treatment techniques [14]. Heat treatment essentially influences the material's microstructure by alleviating the grain refinement structure and related stress in AMMCs. Solutionizing heat treatment in aluminum composites permits the centralization of solidifying solute to separate in the solution [15]. Due to the heat treatment process during quenching, the individual solute particles present in the alloy tend to become single phase while forming a solid solution. The primary objective of quench is to stifle the precipitation amid quenching and to hold solute atoms at vacancies in the solution. The finest blend of solidarity and ductility is accomplished from a fast quench. The rate of cooling was preferred to acquire the ideal microstructure and to lessen the duration while considering certain basic temperatures amid quenching process [16, 17]. The rapid quenching process makes an inundated solution and thereby offers improvement in the mechanical properties of the matrix. High resistance to erosion has been procured through high speeds of quenching [18]. Prabhu Swamy et. al. [19] created AA6061-SiC particle composites utilizing mix throwing strategy and introduced to a solutionizing heat treatment at a required temperature of 530 °C for 60 min; Quenching was done in water, air, and ice. The heat treatment process was found to improve wear and mechanical properties. Reddappa et. al. [20] produced Al6061-Beryl composites, and subjected it to solutionizing heat treatment at a required temperature of 530 °C for a time period of 18 hr and then allowed to ice quench. Ramesh et. al. [21] made Al6061 with frit reinforcement particulate composites and exposed it to solutionizing heat treatment to a required temperature of 530 °C for about 2 h and quenching was done using ice, air, and water. The composites indicated huge upgrades in hardness property. Manjunath et. al. [22] concentrated on outcomes of heat treatment on strength, microstructure, and wear properties of Al6061-fortified carbon nanotubes and subjected to solutionizing heat treatment at a temperature of 555 °C for about 8 h

accompanied by quenching in permeated water. Heat-treated composites indicated better hardness with improved wear resistance when contrasted with base matrix. Keshava murthy et. al. [23] detailed on the impact of heat treatment and thermo-mechanical process on wear attributes of aluminum-based MMCs; heat treatment impacted hardness and wear attributes of composites. Heat-treated composites showed better wear restriction and lower coefficient of friction (COF) and stood apart from the as-cast composites. Among all the different quenching media, samples under ice quench indicated improvement in hardness and wear obstruction was related to the rate of COF [24].

In the current work, AMMCs strengthened with in-situ AlB_2 particulates were prepared by exothermic reaction between halide salt and Al–Si–Mg-based Al6061 matrix utilizing in-situ technique. The prepared composites were fed to solutionized heat treatment with various quenchants like oil, water, and ice and evaluated for wear and mechanical properties.

2 Experimental Procedure

Aluminum 6061 (Al) matrix (Table 1) was utilized as a base material procured from Fenfe metallurgical center, Bangalore, and the fortification salts of KBF_4 (Table 2) utilized as a strengthening material were procured from Madras fluorine plant, Chennai to produce Al6061-AlB_2 in-situ composites.

2.1 Fabrication of in-situ Composites

The Al/AlB_2 in-situ composite was delivered through concoction responses between KBF_4 (analytical purity of 98%) and Al6061 aluminum combination at 850 °C in an electrical resistance heater. A little amount of Na_3AlF_6 salt was additionally included as activator for the substance response. KBF_4 powder was constantly fused into the liquid aluminum combination while being stirred with a graphite rod. Following an hour of response time at 850 °C, the melt was casted into a preheated mold [25–27]. During the stirring process, undesirable slag buoyed over the surface and it was skimmed off, later the softened residue was filled in the preheated cast

Table 2 Chemical composition of KBF_4

Compound	Boron	K_2SiF_6	Fe	Moisture	Balance
%	8.51%	0.84%	0.022%	0.06%	98.9%

Table 1 Al 6061 alloy composition by Mass%

Al	Mg	Si	Fe	Cu	Cr	Zn	Ti	Mn	Remainder
96.84	0.9	0.55	0.5	0.17	0.3	0.24	0.23	0.13	0.14

iron mold. The as-cast and composite samples were separated into little pieces for microstructural examination. The specimens were polished using files, emery paper, and velvet cloth. Subsequent to polishing, the samples were exposed to chemical etching (0.5% HF) and analyzed microscopically using Scanning Electron Microscope (SEM). To recognize the phases, in-situ composite samples were investigated by utilizing an X-Ray diffraction spectrometer (XRD) with Cu-Ka radiation.

A substance response happens between the aluminum melt and calculated amounts of halide salt as follows:

$$3Al + 2KBF_4 \rightarrow AlB_2 + 2KAlF_4.$$
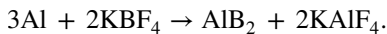
2.2 Heat Treatment

The process of heat treatment technique includes three distinct steps namely solutionizing, quenching, and finally artificial aging. Firstly, the composite is heated to a required temperature of 535 °C for 1 h till the solute components of matrix are broken down until it liquefies completely in the Al6061 strong solution. Then, the samples are immediately quenched in oil, water, and ice and then artificially aged at a temperature of 175 °C for an aging time duration of 10 h. Subsequently, the samples were cooled naturally at room temperature.

2.3 Uniaxial Tensile and Hardness Tests

The tensile tests were completed according to ASTM E8 principles using a computerized hydraulic universal tensile testing machine (UTM) (Model: TUE-C-1000) to find the tensile strength and ductility properties, and the microhardness tests were completed according to the ASTM E384 standard using a Brinell hardness (BHN)testing analyzer (Model: 2004/278) with 500 Kgf load. Three samples were used for each test and the average reading was considered for both the tests.

2.4 Analysis of Wear

A DUCOM pin-on-disc machine having a circumference of 100 and thickness of 10 mm was utilized to assess the specific wear rate on the sliding surfaces of the samples. The disc was made up of HN32 steel. The tests were directed under room temperature conditions according to the ASTM G-99 standard. The pin surface was at first scrubbed with acetone reagent and weighed precisely using computerized electronic weight balance equipment. The test was carried out using normal loads and acted upon sliding distances of 1000 m at three distinctive linear speeds of 1.04, 2.09, and 3.14 m/s. Towards the end of each test condition, the pin

was once again weighed for one more time and subsequently washed with acetone reagent. The distinction between the preliminary weight and final weight was taken into consideration as a proportion of slide mass misfortune.

3 Results

3.1 Microstructure

Figure 1a–d illustrates SEM micrographs of the as-cast and heat-treated composites. The micrographs showed uniform dissemination of grains throughout the area; The SEM image of the as-cast Al6061 shows an average dendritic structure because of solidification. The dendritic structure is formed because of higher cooling rate achieved during hardening. It is portrayed with increased essential α-aluminum dendritic arms [28]. The dendritic arm structures appear to be far less in the microstructures of Al-6 wt% AlB_2 in-situ composites processed with various quenchants as shown in Fig. 1b–d. It is fascinating to note the particle interface between the reinforcement AlB_2 and the Al matrix. Since the interface is plain and constant throughout, and in the absence of smaller scale pores, there are no nasty reaction product items near the interface. The plain interface is a classic quality associated with in-situ process [29]. These qualities of the interface demonstrate that the AlB_2 particles are very much adhered to the aluminum matrix. The particles are combined inside the liquid aluminum by the in-situ chemical reaction. The absence of reactions of undesirable products at the interface affirms that the in-situ-formed AlB_2 particulates were found to be thermodynamically steady with liquid aluminum. There is a mismatch of Coefficient of Thermal Expansion (CTE) between Al base matrix and AlB_2 particles and this results in many dislocations [30, 31]. The particulates are not presented to the atmosphere directly. Along these lines, particulates eventually display unadulterated oxide-free surfaces which give better interfacial holding. Amid reaction with the development of in-situ-formed AlB_2 particles, they can freely suspend in liquid aluminum for a longer period of time. The liquid aluminum starts to wet the AlB_2 particles following the development of particulates by in-situ response. The activity of wetting is assisted with the free movement of AlB_2 particulates. It is additionally expressed that the progression of Al matrix throughout the AlB_2 particles under high tension can enhance the holding strength of AlB_2 particle and composites [32]. The nearby increase in the liquid Al temperature because of in-situ exothermic chemical reaction further guarantees great wettability. Clustering of AlB_2 particulates is seen hardly in any areas in Fig. 1c, d for water and ice quenching.

Figure 1b–d obviously shows the uniform circulation of AlB_2 all through the base matrix and furthermore some

Fig. 1 a–d SEM micrographs of 6061Al-6 wt% of AlB$_2$ composites. **a** as-cast. **b** Oil-quenched composites. **c** Water-quenched composites. **d** Ice-quenched composites

(a)

(b)

(c)

(d)
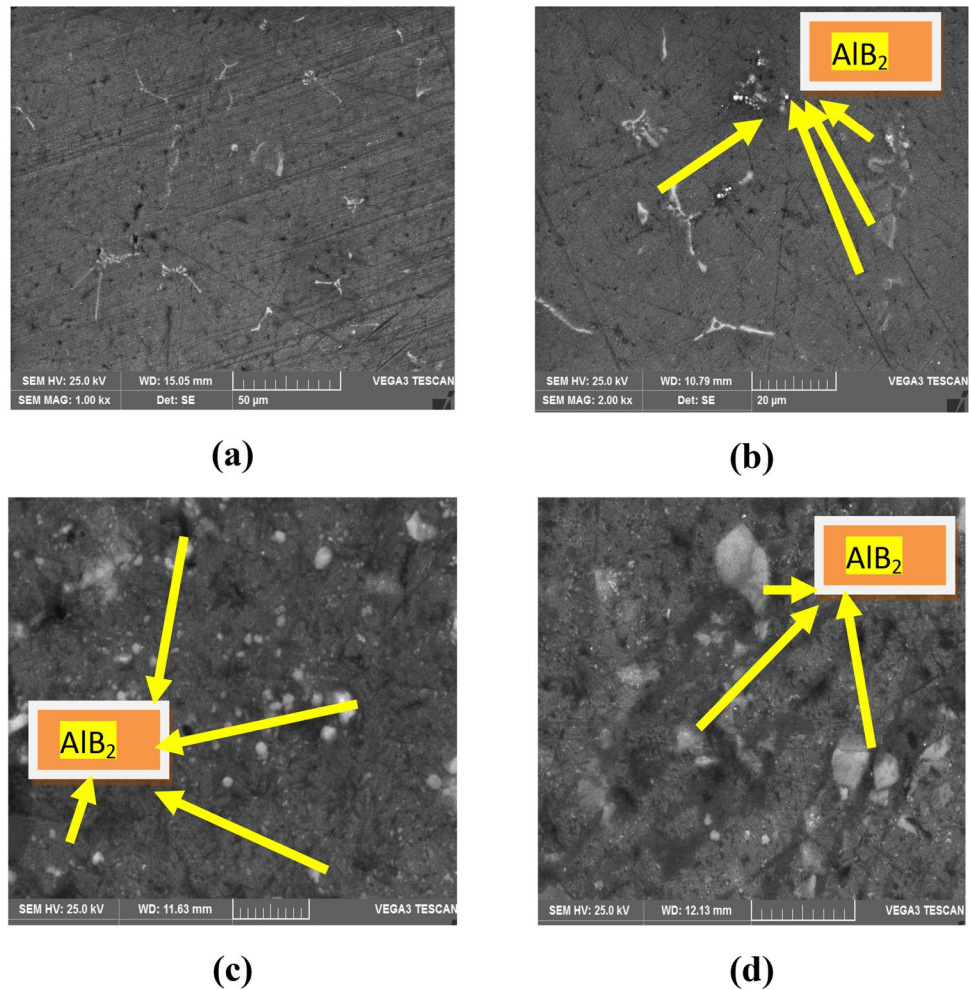
agglomeration at few spots were also seen in composite strengthened with 6 wt% of AlB$_2$ reinforcement. AlB$_2$ particles with various shapes like round and hexagonal are seen in Fig. 1c, d. The fortification has a noteworthy impact on the properties of AMMCs. Figure 1c, d uncovers a uniform circulation of in-situ AlB$_2$ particles with low clustering when compared with Fig. 1a. This is on the grounds that oil quenching is normally termed as a moderate quench. It has a relatively slower cooling rate than ice or water. Distortion and cracking are lower when compared with water or ice. This can be ascribed to the presence of lesser disengagements after oil quenching is done; the Mg$_2$Si particles from the interparticle region do not diffuse altogether and is sufficient to cause early precipitation [33, 34].

3.2 XRD Analysis

To recognize the AlB$_2$ particle phases of the quenched composites, XRD examinations were directed using Cu radiations (*Courtesy: BMSCE and JIT, Bengaluru*) to analyze the Al6061-6 wt% AlB$_2$ particles (Fig. 2). The investigation

is performed using a Philips diffractometer and detailed information is recorded utilizing X'Pert programming information. The composites affirm efficient interface holding between AlB$_2$ particles in the samples.
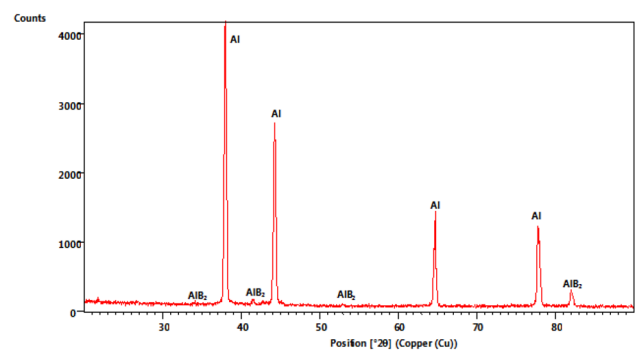

Fig. 2 XRD patterns of Al-6 wt% AlB$_2$ composites

3.3 Mechanical Properties

The mechanical properties of the heat-treated in-situ composites in different quenchants were examined. Each test was completed multiple times and the average value is accounted for in the charts (Fig. 3a, b). The hardness values of the Al-AlB$_2$ composites subjected to heat treatment with various quenchants increase altogether. As can be observed from Fig. 3a, b, the hardness and Ultimate Tensile Strength (UTS) of the in-situ composites subjected to various quenchants are higher than the as-cast composites. Ice-quenched samples showed maximum enhancement in the properties of the in-situ composites followed by water and oil quenching. Similar
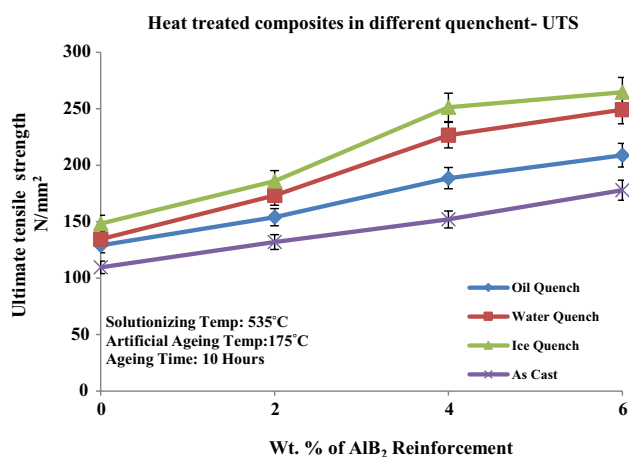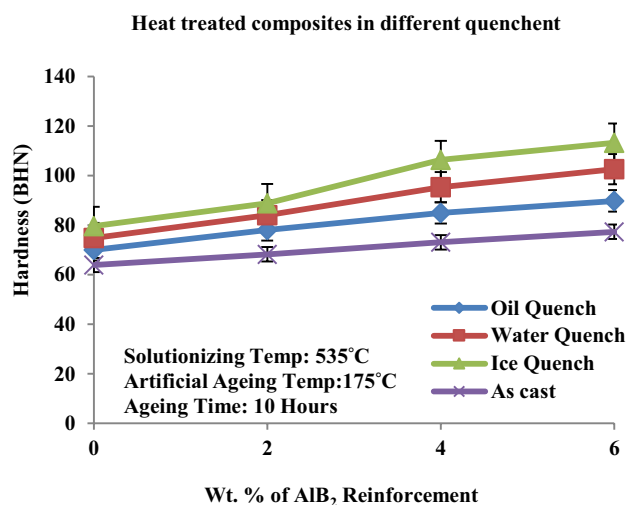

(a)

(b)

Fig. 3 **a** Hardness variation in different quenchants of Al-AlB$_2$ composites. **b** UTS variation in different quenchants of Al-AlB$_2$ composites

trends were observed by other researchers [35, 36]. This is on the grounds that the enormous disfigurement increases the holding strength among in-situ particles and base matrix, and permits the load to successfully move through the Al/AlB$_2$ particle interface.

3.3.1 Hardness

It is clearly observed that in-situ AlB$_2$ particles improve the hardness of the as-cast composites with various quenchants. This is because of the way that the rigid and hard AlB$_2$ particle reinforcement necessitates the plasticity of the delicate matrix amid the hardness strength test. During the hardness test of the as-cast and heat-treated composites, it is understood that plastic deformation causes work-solidifying for most poly-crystalline metals, however, the pressure can be loosened up when the strain increases partially. As the stack deficiency vitality of Al matrix is high, the disengagements can be simpler to move as cross slip. The disengagements can progressively recuperate during the development [37, 38]. Due to this phenomenon, the conditioning rate is more than the solidifying rate, bringing about work mellowing. Appropriately, this conditioning checks work-solidifying. This also reduces the work-solidifying rate.

3.3.2 Tensile Strength

It is observed that tensile strength of the ice quenching specimen shows higher improvements in the UTS when compared with water and oil quenching. From the literature review it was noted that during solidification at higher cooling rates, the Guinier–Preston–Bagaryatsky (GPB) zones open. While the rate of cooling increases, the measure of quenched constraint that is crucial for GPB zone solution also increases. In addition, the density of the composites is the same as the strength of the composites. This combined with the disengagement fortification results in extreme and abrupt increases in the ice quenching of heat-treated samples [35–38]. An alternative reason for the subsequent reinforcing is the cooperation among disengagements and AlB$_2$ particles; when the in-situ composites carry a normal load and furthermore due to the presence of various dislocations through the AlB$_2$ particles as a result of the distinction in CTE mismatch between the as-cast matrix and AlB$_2$ particles, the CTE confound between these particulates within the matrix additionally carry the disengagement reinforcing at grain structure boundary, as per the CTE mismatch. When accumulating along the grain boundary, AlB$_2$ particles cannot add to Orowan fortifying. However, these particles hinder the disengagement slip since they have high bonding strength and hardness. Enormous deformation increases the bonding strength between the in-situ particles and base

matrix and permits the load to viably move by Al/AlB$_2$ particle interface. Very minor particles fill the gaps of huge particles and enhance additional limit of reinforcing [39].

This enhancement in strength might be ascribed to refinement of grains due to the presence of AlB$_2$ particles, which is also in agreement with the Hall–Petch interrelation. Increase in general disengagement density all over the AlB$_2$ particles due to the CTE mismatch of Al base matrix and AlB$_2$ particles amid hardening additionally adds to strength [35–38]. The presence of halide cryolite salt in the in-situ composites makes uniform appropriation of AlB$_2$ particles in the matrix and thereby reducing clustering amid reaction.

3.3.3 Effect of Various Quenchants on Mechanical Properties

Figure 3a, b reveals the mechanical properties of composites quenched in various media. The most improved hardness and UTS in the composites were observed with the ice quenching process followed by water and oil. This can be exclusively because of higher quenching rate by ice since the time given for strain unwinding is generally less. The significance of interfacial zone and augmentations in disengagement density is another purpose behind the increase in hardness. Different factors which may influence expansion during quenching are particle size, measure of reinforcement, and response temperature. The decrease in hardness for sample without experiencing heat treatment and quenching may be a direct result of weak interfacial holding between the AlB$_2$ particles and aluminum matrix. Ice and water quench samples set apart longer efforts to attain higher hardness and UTS values which are exposed to aging treatment. More detachments are produced at the particle–matrix interface because of their CTE befuddle when compared with the matrix–particle locale. This causes Mg bits from the matrix to diffuse through the interfacial locale. The centralization of Mg particles in the matrix diminishes and hence precipitation is deferred and thereby shows high hardness at higher aging times. Ice-quenched samples show maximum hardness when opposed to water and oil-quenched samples. Oil is graded as an intermediate quench. It has relatively slower cooling rate than water. Oil-quenched sample shows improved hardness during the initial phase of aging. This can be ascribed to the existence of lesser disengagements after oil quenching, with the goal that the Mg particles from the inter-particulate area do not diffuse fundamentally and their fixation is sufficient to cause early precipitation [39, 40].

Subsequently, the in-situ AlB$_2$ particles have uniform dispersion and grouping as shown in Fig. 1a. In oil quenching, in view of high density of oil, the fume spread gets drawn out achieving lower cooling rate. This generally diminishes the density. Bringing down the density of oil at high temperature results in overhauled cooling rate. The higher sluggish

heat of vaporization of oil achieves lower cooling potential. When required temperature is extended to 175 °C, hardness values were viewed to be intensifying with increasing weight % of AlB$_2$ particles. The density of oil is decreased at high temperatures and as such, quench impact is improved. More displacements are delivered which are impeded by the AlB$_2$ particles having progressive resistance effect [19–22, 41, 42]. Ice and water-quenched samples creates a bigger number of disengagements than oil-quenched samples. Oil is found to be a less severe quenching medium; it creates less loads thus hardness is least. It is thus presumed that when the specimens were heat-treated and quenched, countless number of dislocations are assembled because of the mismatch in CTE between the AlB$_2$ particulates and matrix.

3.4 Wear Properties

The reinforcement rate influences the wear sliding speed and sliding distance of the composite specimens. It is noted that the wear rate of the composites diminishes with expanding content of AlB$_2$ particle reinforcement in the as-cast compound but for a specific wt% of reinforcement, the in-situ composites have lower wear rate than as-cast samples subjected with various quenchants. The increased wear opposition of the composites with expanding substance of in-situ AlB$_2$ reinforcement can be ascribed to the increase in the hardness strength of the composite material [11–13, 40, 43]. The other persuasive parameter on the wear rate is the sliding rate and distance.

3.5 Load with Volumetric Wear (Vw)

Figure 4a–c shows the details about the rate of volumetric wear (Vw) at different loads associated with a sliding distance of 1000 m and at a dependable steady sliding speed of 300 rpm. It shows increase in wear rate with increasing test loads while maintaining a constant sliding distance of 1000 m. This is due to the growth in the friction pressure between the particle interface of sample and steel counterface. This is attributed to the scouring activity created between the matrix composite specimens and sliding surface. When a maximum load of 49.03 N is used, the wear rate is much higher and this is because of the adhesive and ploughing action on the surface of the specimens. At this stage, the contact friction pressure between the surface of the composite and steel counterface is more, which is the outcome of higher wear. In all the distinctive quenchants, ice-quenched composites showed great wear obstruction followed by water and oil. This is a direct result of aging treatment in ice quenching, and more disengagements are produced at the particle–matrix interface because of their CTE mismatch when contrasted with the interparticle area [13, 22–24, 43].
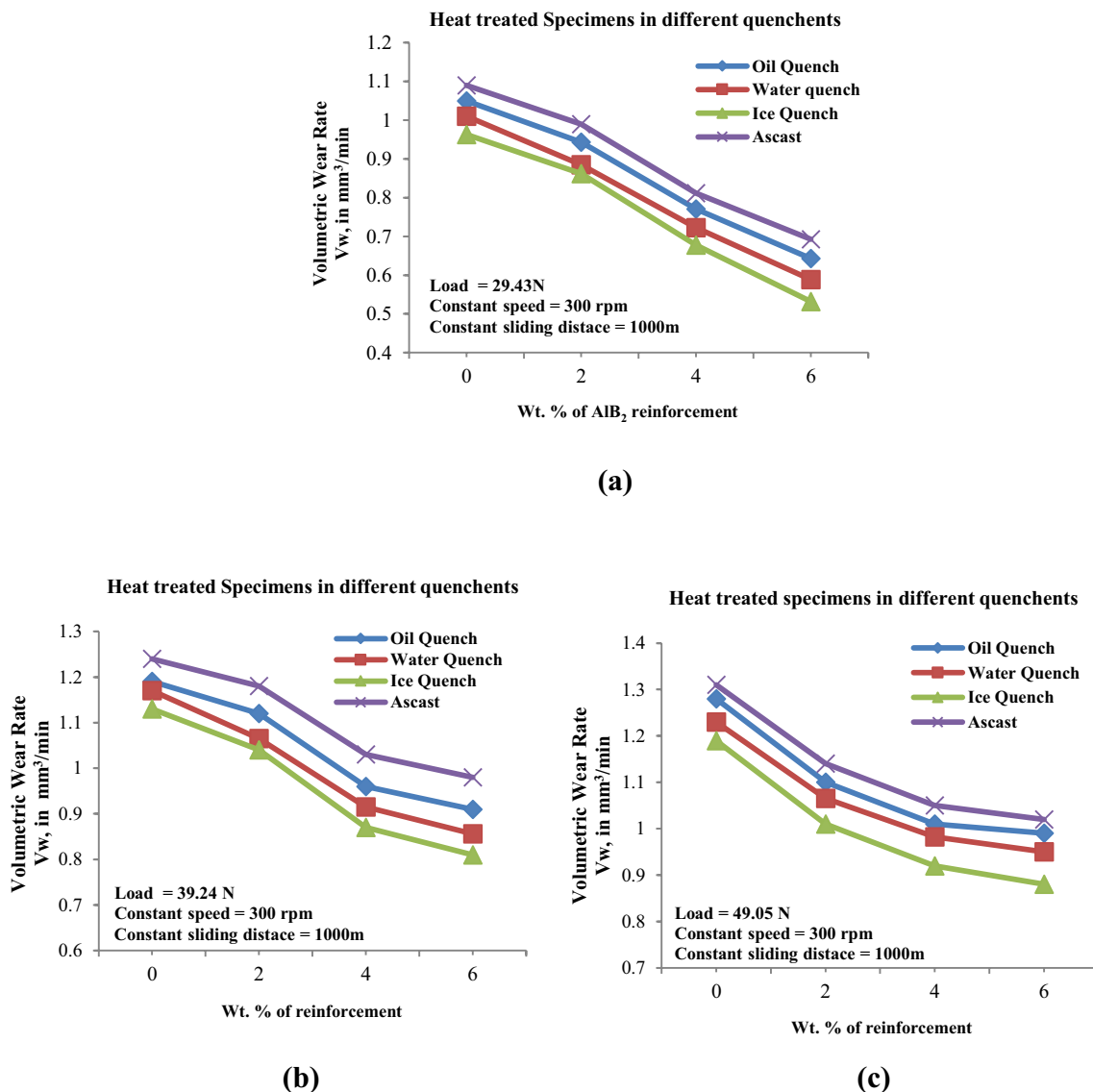
Heat treated Specimens in different quenchents

(a)

Heat treated Specimens in different quenchents

(b)

Heat treated specimens in different quenchents

(c)

Fig. 4 **a–c** Volumetric wear rate of heat-treated in-situ composite in different quenchants of Al-AlB$_2$ composites for various loads; at sliding speed of 300 rpm and distance of 1000 m

It is observed that the volumetric wear rate of the as-cast composites is high when compared with the heat-treated samples. This might be due to the aging treatment time for the strain unwinding during quenching and precipitation owing to the presence of Mg particles in the encompassed region. The material undergoes high plastic deformation under higher associated load. At a load of 49.05 N due to excessive prominent plastic twisting, the odds of sub-surface break are high which cause high wear disaster. This is chiefly a direct result of high quenching speed by ice since time given for unwinding for strain rate is exceptionally less in ice quenching when compared with oil and water-quenched samples, further aluminum diboride bolsters in the matrix and enormously impacts volumetric wear rate. Reduction

in the wear rate of Al-6 wt% AlB$_2$ composite in different quenching media is associated with the presence of AlB$_2$ in the composites with aging treatment [43, 44].

3.5.1 Sliding Speed with Volumetric Wear

From Fig. 5a–c, variation in volumetric wear rate is seen when the sliding speed differs from 100 to 300 rpm. At the point when the sliding speed is 100 rpm, the wear rate of the oil-quenched composites is high because of serious delamination of severities on the composite surface created by sliding activity when contrasted with water and ice-quenched samples. Wear rate increases when the sliding speed is varied from 200 to 300 rpm, and movement and
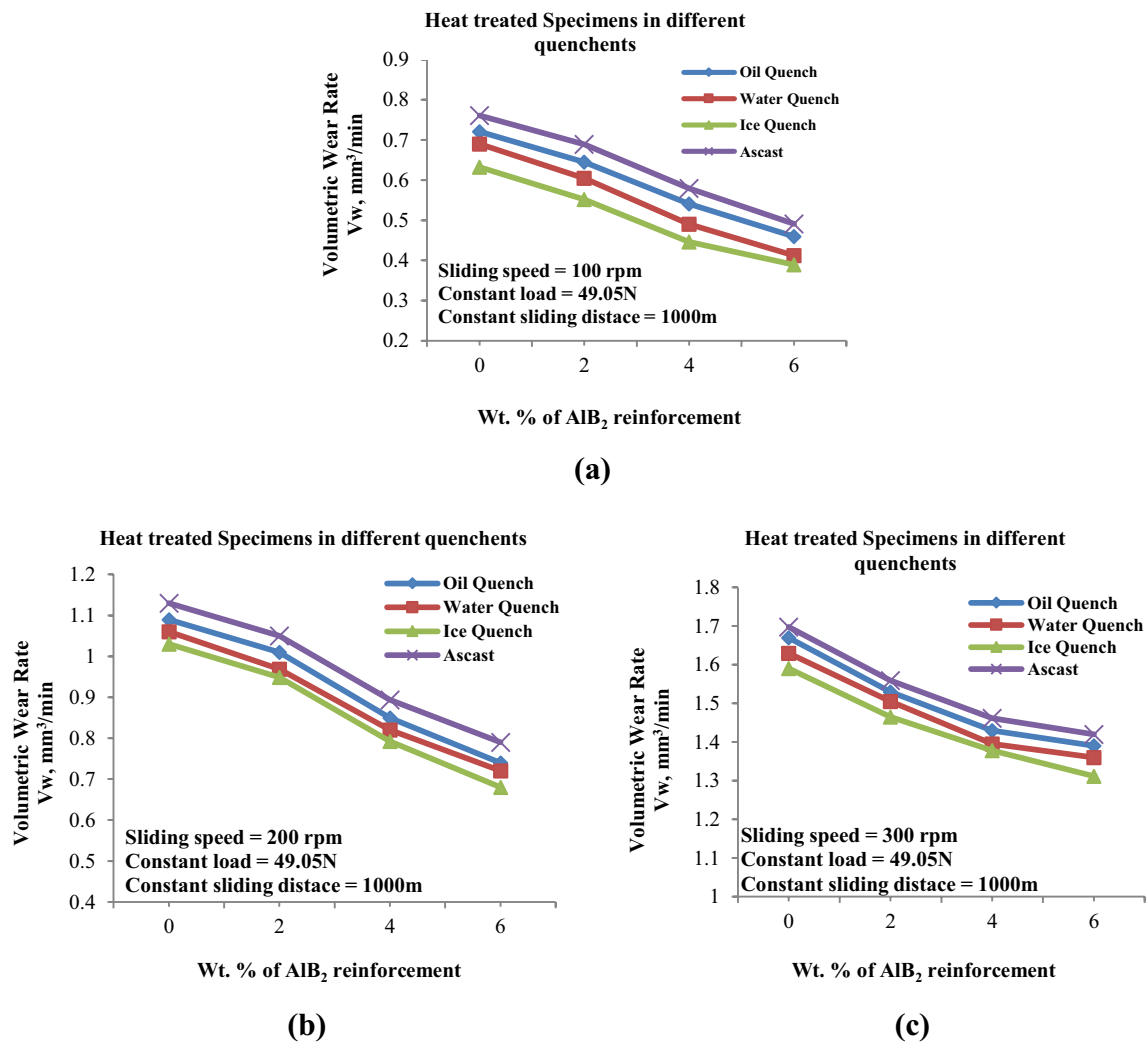
Heat treated Specimens in different quenchents

Oil Quench
Water Quench
Ice Quench
Ascast

Sliding speed = 100 rpm
Constant load = 49.05N
Constant sliding distance = 1000m

Wt. % of AlB$_2$ reinforcement

(a)

Heat treated Specimens in different quenchents

Oil Quench
Water Quench
Ice Quench
Ascast

Sliding speed = 200 rpm
Constant load = 49.05N
Constant sliding distance = 1000m

Wt. % of AlB$_2$ reinforcement

(b)

Heat treated Specimens in different quenchents

Oil Quench
Water Quench
Ice Quench
Ascast

Sliding speed = 300 rpm
Constant load = 49.05N
Constant sliding distance = 1000m

Wt. % of AlB$_2$ reinforcement

(c)

Fig. 5 **a–c** Volumetric wear rate with wt% of reinforcement with various quenchants of Al-AlB$_2$ in-situ composites for various sliding speeds and fixed sliding distance of 1000 m at a load of 49.05 N

material transfer happens during this condition due to continuous sliding and this forms a layer of wear debris [25–27, 44]. Moreover, oxide layer is developed because of increase in temperature at the interface, which decreases the rate of wear. At this high sliding speed, the interface temperature turns out to be higher and the interfacial holding strength becomes weak and the in-situ AlB$_2$ particles of the wear debris get separated by the sliding activity [42–44].

Figure 5a–c speaks about the progressions in volumetric wear rate for sliding speeds of 100, 200, and 300 rpm, sliding distance of 1000 m, and at a consistent normal load of 49.05 N. The wear rate increases gradually as the sliding velocity increases in all the quenchant media used. Initially, the sample surface is glided and long sections are cut onto it. Likewise, the heat produced due to friction is high at higher rates of sliding velocities, which causes the rise of surface temperature in the samples. At high temperatures, the plastic

distortion of sample material increases at the surface and sub-surface. This is due to the plastic progression of material which occurs at high temperatures due to which few fragments of the surface are moved causing distension. Nonetheless, the diminished wear rate in the developed composites is basically a result of the presence of AlB$_2$ particulates on the surface of samples which slides with the counterface amid sliding [28, 29]. The in-situ AlB$_2$ particulates are found to resist the spread of cracks amid sliding wear because of the dislocations during hardening, due to thermal CTE mismatch between aluminum matrix and AlB$_2$ particles [40, 44].

3.5.2 Sliding Distance on Wear Rate

At a sliding distance (SD) of 1000 m, the wear rate is high in oil-quench media due to the hard severities projecting

from the in-situ composite. The surface gets in friction contact with steel counterface and breaks because of the sliding activity [29, 31–33, 44–47]. The hard asperities from the in-situ composite surface get softened and uniform friction contact between the composites surface and the steel counterface is achieved. The impact of the sliding distance upon wear rate, in any case, is much lower when compared with the sliding speed and amount of fortification inside the composites [26, 27].

3.5.3 Worn Surface Characterization Using SEM

Impact of AlB_2 particle reinforcement and heat treatment on the structure of the worn surface of composite are as shown in Fig. 6a–i. Utilizing SEM, wear surface investigation of in-situ AlB_2 particle composites is analyzed under test conditions of 49.03 normal load, sliding rate of 300 rpm, and sliding distance of 1000 m. Oil-quenched samples (Fig. 6a–c) with various reinforcements of AlB_2 have furrowing impact
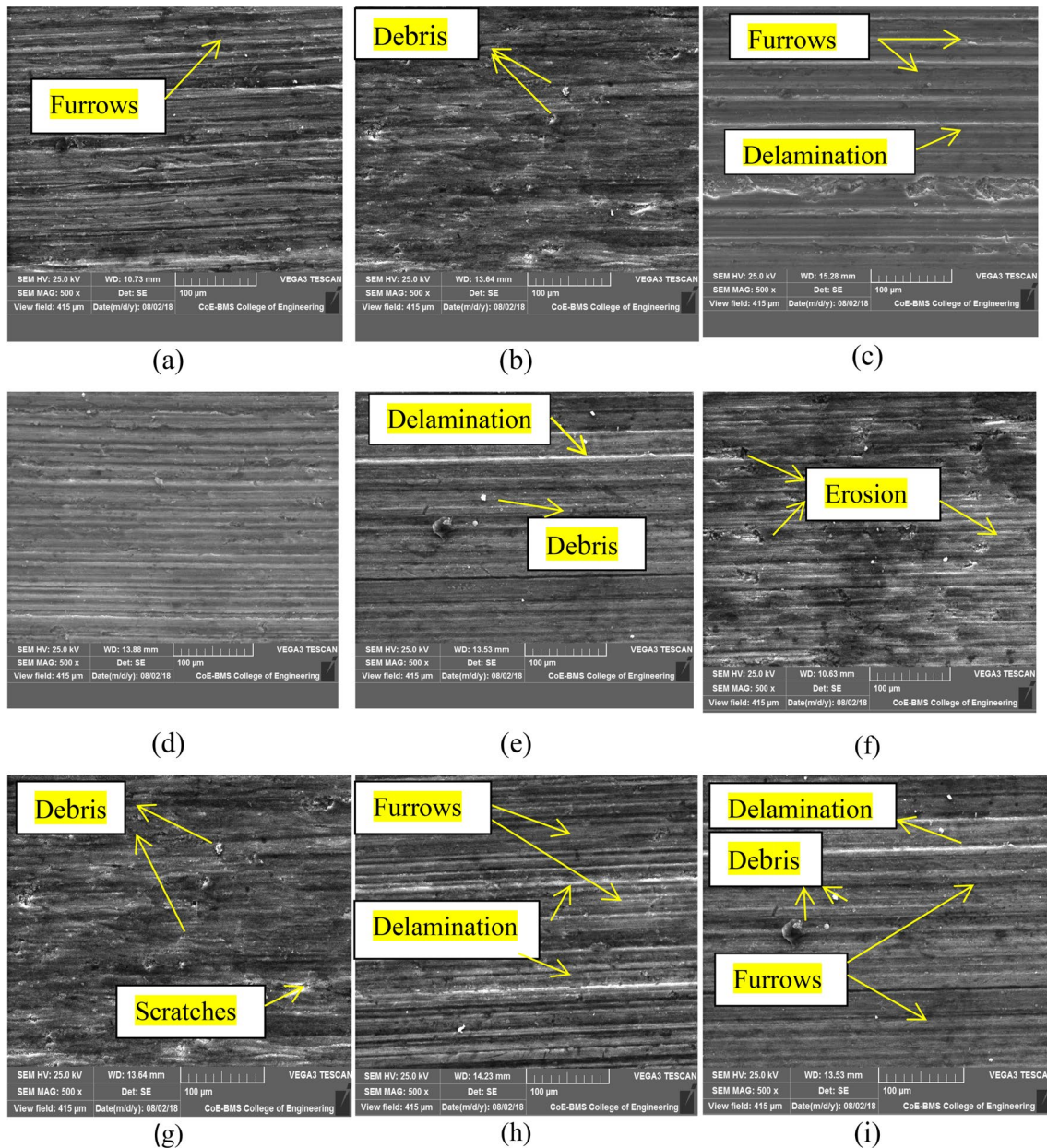

Fig. 6 **a–i** SEM micrographs of heat-treated Al-AlB_2 composites with different quenchants under applied load 49.05 N, sliding speed 300 rpm, and sliding distance 1000 m. (1) Oil Quench **a** Al6061-2wt% AlB_2 **b** Al6061-4wt% AlB_2 **c** Al6061-6wt% AlB_2. (2) Water Quench **d** Al6061-2wt% AlB_2 **e** Al6061-4wt% AlB_2 **f** Al6061-6wt% AlB_2. (3) Ice Quench **g** Al6061-2wt% AlB_2 **h** Al6061-4wt% AlB_2 **i** Al6061-6wt% AlB_2

on the counter disc and increasing number of fortification particles are observed on a superficial level. The high delamination formed removes the material and the above perceptions are utilized as the wear rate is higher for a sliding speed of 300 rpm. Worn surface of oil-quenched base matrix shows the presence of profound furrows due to substantial plastic deformation.

Figure 6d–i depicts the SEM microphotographs of worn surface of water and ice-quenched samples that obviously show scant scraped area grooves when contrasted with the depressions of oil-quenched samples. Further, the harder AlB_2 in-situ particles depict less splits and damage in worn surfaces. More scores and reinforcement AlB_2 particles are observed in Fig. 6f in water-quenched sample showing the expansion of wear rate with increase in load for the equivalent sliding speed. Figure 6g–i shows shallow scratches, least scores, and delamination uncovers with less wear rate due to ice quenching. This is due to the presence of harder AlB_2 particulates in the composite which carry the load on the as-cast matrix surface and shows further decrease in groove size and splits due to the presence of higher measure of hard AlB_2 particles with the increase in reinforcement content [27–29, 45].

Due to the presence of fine oxide particulates, oxidation and abrasive wear is observed [27]. Oxide particles are fundamentally formed because of the heat produced by erosion while sliding on the counter steel disc. The presence of oxide particles alongside harder AlB_2 particulates is responsible for lesser wear rate in Al-6 wt% in-situ AlB_2 composites.

4 Conclusions

The current examination concludes that:

1. AMMCs strengthened with in-situ AlB_2 particles were effectively fabricated by vortex course using in-situ strategy.
2. The microstructure of in-situ composites shows that AlB_2 is consistently circulated with different morphologies in the matrix and affirmed with SEM and XRD studies.
3. Tensile and hardness strength of the in-situ composites increases with increasing wt% of the reinforcement and further infers that both hardness and tensile strength expanded with ice quench followed by water and oil quenching.
4. The composites showed improvement in wear resistance fundamentally because of the development and distribution of in-situ AlB_2 particles in the matrix. Wear increased directly with the expansion in applied load in all the quench media.

5. Irrespective of the quenching, the volumetric wear rate of Al-6 wt% AlB_2 composites is lower when compared with the composites with 2 and 4 wt%-reinforced AlB_2 composites. This is because of the presence of AlB_2 particles in the composites. Ice-quenched composite samples showed less volumetric wear rate when compared with water and oil-quenched samples.
6. Worn surface examinations conducted in various quenchants using SEM have revealed rough and oxidative wear behavior in AlB_2-strengthened in-situ composites. It is observed that ice-quenched samples have less number of furrows or notches when compared with water and oil-quenched samples.

References

1. Pramod SL, Bakshi SR, Murty BS (2015) Aluminum-based cast in situ composites: a review. J Mater Eng Perform 24:2185–2207
2. Dayanand S, Satish Babu B (2020) A Review on synthesis of AlB_2 reinforced aluminium matrix composites. IOP Conf Ser Mater Sci Eng 810:012038. https://doi.org/10.1088/1757-899X/810/1/012038
3. Reddy BSB, Das K, Das S (2007) A review on the synthesis of in situ aluminium based composites by thermal, mechanical and mechanical-thermal activation of chemical reactions. J Mater Sci 42:9366–9378
4. Boppana SB, Dayanand S (2020) Development of AlB_2 particles using inorganic halide salts and mechanical characterization of AlB_2 reinforced AA6061 MMC's. Mater Today Proc 27:595–602. https://doi.org/10.1016/j.matpr.2019.12.068
5. Boppana SB, Dayanand S, Anil Kumar MR, Kumar V, Aravinda T (2020) Synthesis and characterization of nano graphene and ZrO_2 reinforced Al 6061 metal matrix composites. J Mater Res Technol 9(4):7354–7362. https://doi.org/10.1016/j.jmrt.2020.05.013
6. Boppana S, Chennakeshavalu K (2009) Preparation of Al-5Ti master alloys for the in-situ processing of Al-TiC metal matrix composites. J Minrls Mater Char Engg 8(7):563–568. https://doi.org/10.4236/jmmce.2009.87049
7. Boppana S (2020) In situ synthesis of titanium carbide in pure aluminium. J Mater Sci Chem Engg 8:1–10. https://doi.org/10.4236/msce.2020.81001
8. Hoseini M, Meratian M (2009) Fabrication of in situ aluminium-alumina composite with glass powder. J Alloys Compd 471:378–382
9. Karantzails AE, Lekatou A, Gerogties M, Poulas V, Mavros H (2011) Casting based production of Al-TiC-AlB_2 composite material through the use of KBF_4 salt. J Mater Engg Perform 20(2):198–202
10. Wang X (2005) The formation of AlB_2 in an Al- B master alloy. J Alloys Compd 403:283–287

11. Maldovan P, Dragut DV (2015) In-situ productions of Al/AlB$_2$ composite by metal salt reaction. Research gate net publication. https://doi.org/10.13140/RG2.1.1339.5367

12. Boppana SB, Dayanand S, Ramesh S (2020) Effect of reaction holding time on synthesis and characterization of AlB$_2$ reinforced Al6061 metal matrix composites. J Bio Tribo Corros 6:88. https://doi.org/10.1007/s40735-020-00385-4

13. Kayikcia R, Savas OB, Koksala S, Demira A (2013) The effect of reinforcement ratio on the wear behaviour of AlB$_2$ flake reinforced MMCS. Acta Phys Pol, A 2(125):24–28

14. Queyreau S, Monnet G, Devincre B (2010) Orowan strengthening and forest hardening superposition examined by dislocation dynamics simulations. Acta Mater 58:5586–5595

15. Shabestari SG, Shahri F (2004) Influence of modification, solidification conditions and heat treatment on the microstructure and mechanical properties of A356 aluminum alloy. J Mater Sci 39:2023–2032

16. Pedersen L, Arnberg L (2001) The effect of solution heat treatment and quenching rates on mechanical properties and microstructures in Al-Si-Mg foundry alloys. Metall Mater Trans 32A:525–532

17. Dorward RC (1997) A dynamic quench model for strength predictions in heat-treatable aluminum alloys. J Mater Process Tech 66:25–29

18. MacKenzie DS, Newkirk JW (2001) The use of the jominy end quench for determining optimal quenching parameters in aluminum. Proceedings of the 8th Seminar of IFHTSE, Dubrovnik, Croatia 12–14 September. p 139

19. Prabhu Swamy NR, Ramesh CS, Chandrashekar T (2010) Effect of heat treatment on strength and abrasive wear behaviour of Al6061SiC p composites. Bulletin Mater Sci 33(1):49–54. https://doi.org/10.1007/s12034-010-0007-y

20. Reddappa HN, Suresh KR, Niranjan HB, Satyanarayana KG (2011) Dry sliding friction and wear behavior of Aluminum/Beryl composites. Inter J Appl Eng Res 2:2

21. Ramesh D, Swamy RP, Chandrashekar TK (2012) Role of heat treatment on Al6061- frit particulate composites. J Miner Mater Char Eng 11(4):353–363

22. Manjunatha LH, Dinesh P (2013) Studies on effect of heat treatment and water quench age hardening on microstructure, strength, abrasive wear behaviour of Al6061-MWCNT metal matrix composites. J Acad Indus Res 1(10):595–600

23. Keshavamurthy R, Madhu Sudhan J, Gowda N, Ananda Krishna R (2016) Effect of thermo-mechanical processing and heat treatment on the tribological characteristics of Al based MMC's. IOP Conf Ser Mater Sci Eng 149:012118. https://doi.org/10.1088/1757-899X/149/1/012118

24. Koksal S, Ficici F, Kayikci R, Savas O (2012) Experimental investigation of dry sliding wear behaviour of insitu AlB2/Al composite based on taguchi's method. Mater Des 42:124–230. https://doi.org/10.1016/j.matdes.2012.05.048

25. Dayanand S, Satish Babu B, Auradi V (2018) Experimental investigation of microstructure and dry sliding wear behavior of Al-AlB$_2$ metal matrix composites. Mater Today Proc 5(10):22536–22542. https://doi.org/10.1016/j.matpr.2018.06.625

26. Dayanand S, Boppana SB, Hemanth J, Aravinda T (2019) Microstructure and corrosion characteristics of in situ aluminum diboride metal matrix composites. J Bio Tribo Corros 5:60. https://doi.org/10.1007/s40735-019-0250-8

27. Boppana SB, Dayanand S (2020) Impact of heat treatment on mechanical, wear and corrosion behaviour of in situ AlB$_2$ reinforced metal matrix composites produced by liquid metallurgy route. J Bio Tribo Corros 6:33. https://doi.org/10.1007/s40735-020-0324-7

28. Savaş O (2012) Application of taguchi method to investigate the effect of some factors on in-situ formed flake structures of Al/AlB$_2$ composite. Adv Compos Lett 21(2):49

29. Ferrict F (2011) Investigation of unlubricated sliding wear behaviour of in situ AlB$_2$–Al metal matrix composite. Adv Compos Lett 20:4

30. Elecicek H, Savas O, Aydin Z, Ozdemir OK, Kayikci R (2015) Corrosion behavior of inistu AlB$_2$/Al-Cu metal matrix composites. Acta Physia Polonica A 129(4):661–664

31. Youn L, Han J, Liu J, Jiang Z (2016) Mechanical properties and tribological behaivour of aluminium matrix composites reinforced with inistu AlB$_2$ particles. Tribol Inter 98:41–47. https://doi.org/10.1016/j.triboint.2016.01.046

32. Radhika N, Raghu R (2016) Effect of abrasive medium on wear behavior of Al/AlB$_2$ functionally graded aluminium matrix composites. Tribology Japan Soc Tribo 11(3):487–493

33. Dumitru (2011) Characterization of in situ AA6061/AlB$_2$ metal matrix composite. U.P.B.SCI.BULL., Series B, 73(1454–2331)

34. Auradi V, Kori SA (2008) Influence of reaction temperature for the manufacturing of Al-3Ti and Al-3B master alloys. J Alloys Compd 45:147–156

35. Anwarkhan AR, Ramesh CS, Ramachandra A (2002) Heat treatment of Al6061-SiC composites. Proceedings of international companies on manufacturing. ICM, Dhaka, pp 21–28

36. Hansen N (2004) Hall-Petch relation and boundary strengthening. Scripta Mater 51(8):801–806

37. Cottu JP, Couderc JJ, Viguier B, Bernard L (1992) Influence of SiC reinforcement on precipitation and hardening of a metal matrix composite. J Mater Sci 27:3068–3074

38. Zhang Z, Chen DL (2008) Contribution of Orowan strengthening effect in particulate reinforced metal matrix nanocomposites. Mater Sci Eng A 483:148–152

39. Rajesh AM, Kaleemulla MK, Doddamani S (2019) Effect of heat treatment on wear behavior hybrid aluminium metal matix composites. Tribo Indus 41(3):344–354

40. Bhat S, Mahesh BS (2014) Effect of heat treatment on microstructure and mechanical properties of Al-FA-SiC hybrid MMCS. Inter J Innov Res Sci Eng Tech 3:6

41. Rajan TV, Sharma CP, Sharma A (1998) Heat treatment principles techniques. Rajkamal Electric Press, Delhi

42. Ramesh CS, Ahamed A, Channabasappa BH, Keshavamurthy R (2010) Development of Al 6063-TiB$_2$ in situ composites. Mater Des 31:2230–2236

43. Gautam G, Mohan A (2015) Effect of ZrB$_2$ particles on the microstructure and mechanical properties of hybrid (ZrB$_2$+Al$_3$Zr)/AA5052 in situ composites. J Alloys Compd 649:174–183

44. Zhang SL, Zhao Y, Chen G, Cheng XN, Huo XY (2008) Fabrication and dry sliding wear behavior of in situ Al-K$_2$ZrF$_6$-KBF$_4$ composites reinforced by Al$_3$Zr and ZrB$_2$ particles. J Alloy Compd 450:185–192

45. Dinaharan I, Murugan N, Parameswaran S (2011) Influence of in situ formed ZrB$_2$ particles on microstructure and mechanical properties of AA6061 metal matrix composites. Mater Sci Eng A 528:5733–5740

46. Golshahr A, Elango Natarajan MS, Santhosh R, Sasikumar SR, Durairaj R (2018) Multi wall carbon nanotube reinforced silicone for aerospace applications. Int J Mech Prod Eng Res Dev 8(4):743–752

47. Ramesh S, Govindaraju N, Suryanarayan CP (2018) Investigation on mechanical and fatigue behaviour of aluminium based SiC/ZrO$_2$ particle reinforced MMC. IOP Conf Ser Mater Sci Eng 346:012030